



# Pollution assessment of the Red Sea-Gulf of Aqaba seawater, northwest Saudi Arabia

Abdelbaset S. El-Sorogy · Mohamed Youssef

Received: 23 August 2020 / Accepted: 26 January 2021 / Published online: 23 February 2021  
© The Author(s), under exclusive licence to Springer Nature Switzerland AG part of Springer Nature 2021

**Abstract** The water pollution index (PI<sub>j</sub>), degree of contamination (C<sub>d</sub>), heavy metal pollution index (HPI), and statistical analyses were used to assess seawater pollution and identify the possible sources of heavy metals from the Red Sea-Gulf of Aqaba coastline, northwest Saudi Arabia. Concentrations of Cr, Sb, Co, Ni, Cu, Zn, Cd, As, Fe, Mn, Hg, and Pb were analyzed and interpreted in 33 surface seawaters samples. The mean heavy metals of seawater were in the following order: Zn (5.51 µg/l) > Ni (2.45) > As (2.43) > Cu (2.34) > Mn (2.20) > Fe (1.81) > Pb (1.31) > Sb (0.64) > Co (0.31) > Cr (0.26) > Cd (0.05) > Hg (0.008). The spatial distribution of heavy metals showed high levels in some individual samples, especially nearby the residential cities, may be due to anthropogenic sources. PI<sub>j</sub> and C<sub>d</sub> indicated light and low pollution for the seawater samples, respectively, while HPI indicated low pollution for 10 samples and medium pollution for the rest ones. The lack of

significant correlations between metal pairs (except Cu and As) indicated different sources of pollution. Pollution indices, principal component analysis, and Pearson's correlation coefficient reveal that the quality of seawater in the Red Sea-Gulf of Aqaba coastline is mainly controlled by geogenic processes with minor anthropogenic input.

**Keywords** Pollution assessment · Heavy metal sources · Red sea · Gulf of aqaba · Saudi arabia

## Introduction

Heavy metals (HMs) are well-known public health significance due to their toxicity, bioaccumulative nature, and persistence in the environment (Ali et al., 2019). Their natural sources include weathering of metal-bearing rocks and volcanic eruptions, while anthropogenic sources include multiple industrial, agricultural, medical domestic, and technological applications (Kabata-Pendias, 2011; Tchounwou et al., 2012; Ali et al., 2019; Kahal et al., 2020). Freshwater and marine ecosystems are vulnerable to pollution by heavy metals from different sources, even at very low concentrations (Akif et al., 2002; Rezaia et al., 2016; Ali et al., 2019). HMs present mainly as suspended colloids or are fixed by organic and mineral substances (Dossis & Warren, 1980; Shi et al., 2020).

Pollution of water bodies has turned increasingly serious by development of the urban economy and increasing urban population year by

---

A. El-Sorogy (✉) · M. Youssef  
Geology and Geophysics Department, College of Science,  
King Saud University, Riyadh, Saudi Arabia  
e-mail: elsorogyabd@yahoo.com

M. Youssef  
e-mail: asmohamed@ksu.edu.sa

A. El-Sorogy  
Geology Department, Faculty of Science, Zagazig  
University, Zagazig, Egypt

M. Youssef  
Geology Department, Faculty of Science, South Valley  
University, Qena, Egypt

year (Qin et al., 2014; El-Sorogy & Attiah, 2015; Alharbi et al., 2017; Shi et al., 2020). The pollution problems of the urban water need urgently solving due to producing large amounts of domestic wastewater, and the industrial areas are concentrated in the suburbs (Shi et al., 2020). Because HMs can bind to suspended matter and accumulate in sediments, and reach toxic levels in a short period, they pose problems for aquatic life and human health (Bozkurt et al., 2014; Lian et al., 2019).

HMs have been increasingly discharged into the coastal environments of the Red Sea and Gulf of Aqaba coasts through human activities by oil spills, effluents of desalination plants, wastewater discharge, and marine traffic (Badr et al., 2009; Lourião-Cabanaet et al., 2011; Pan et al., 2011; Al-Taani et al., 2014; Al-Sofyani et al., 2014; Ghandour et al., 2014; Youssef & El-Sorogy, 2016; Kahal et al., 2018, 2020; Al-Mur et al., 2017; Karuppasamy et al., 2019;

Youssef et al., 2020; El-Sorogy et al., 2020). In their study on contamination and ecological risk status of HMs in the Red Sea-Gulf of Aqaba coastal sediments, El-Sorogy et al., (2020) revealed some anthropogenic inputs with Cu, Cd, Hg, and to a great extent with As. Moreover, they indicated a considerable risk for Cd, Hg, and As. Therefore, the main purposes of the present study are to present the spatial distribution of HMs in seawater in the Red Sea-Gulf of Aqaba coastline, Saudi Arabia, and to document the pollution assessment in the investigated coastal area using water pollution index (PI<sub>j</sub>), degree of contamination (C<sub>d</sub>), heavy metal pollution index (HPI), and statistical analyses.

## Material and methods

The study area extends between Sharma city on the Red Sea coast, at 28° 01' 45" N, 35° 12' 53" E and Maqnah

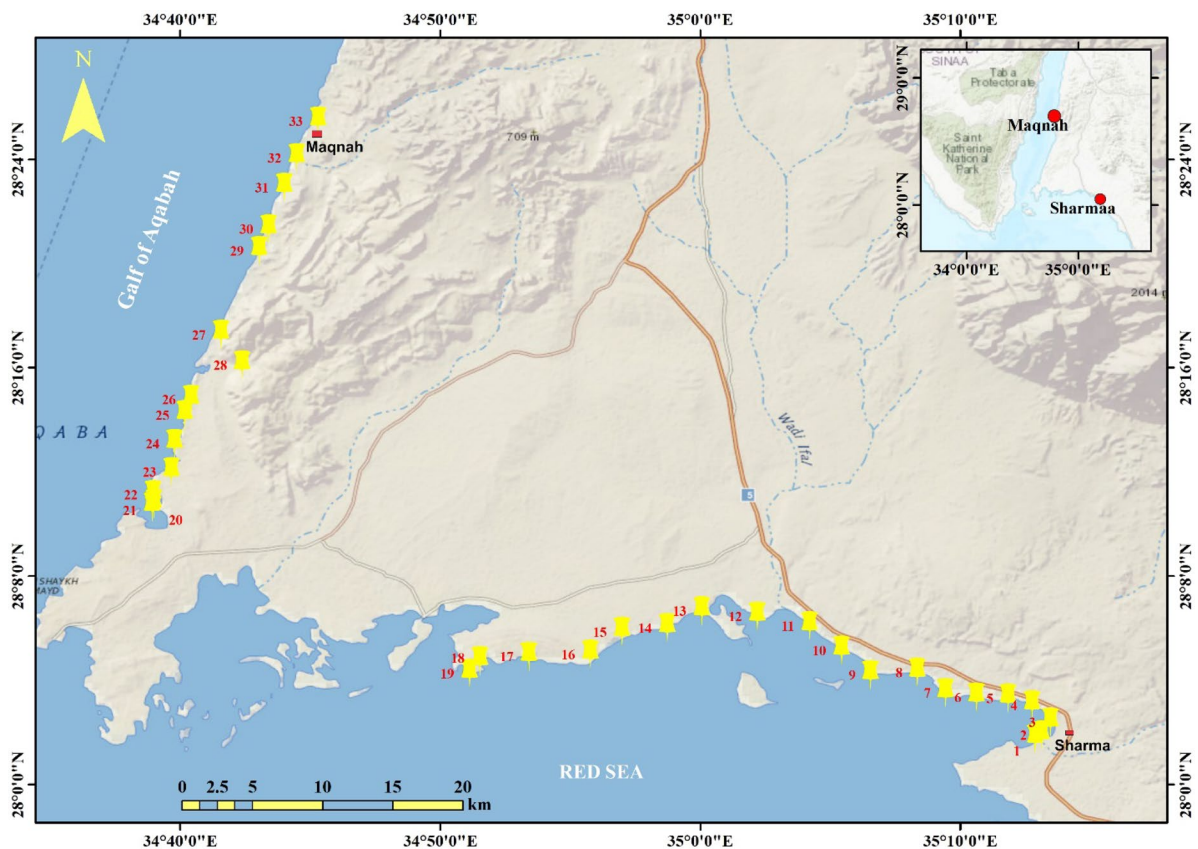


**Fig. 1** Location map of the Red Sea-Gulf of Aqaba coastline and the locations of the seawater samples

**Table 1** The minimum, maximum, mean, and standard deviation of HMs, maximum admissible concentration (Siegel 2002; WHO 2011), and pollution indices in the investigated seawater samples

	As	Cd	Co	Cr	Cu	Fe	Hg	Mn	Pb	Sb	Zn	Ni	PI <sub>j</sub>	C <sub>d</sub>	HPI
Min	1.1	0.04	0.2	0.09	1.1	1.1	0.003	0.68	1	0.3	2.8	1.1	2.01	1.95	4.31
Max	3.8	0.07	0.42	0.43	3.4	2.8	0.013	3.92	1.8	1	8.2	3.8	4.22	2.91	6.78
Mean	2.43	0.05	0.31	0.26	2.34	1.81	0.008	2.20	1.31	0.64	5.51	2.45	3.15	2.41	5.32
St. Dev	0.72	0.01	0.06	0.10	0.68	0.49	0.002	0.74	0.20	0.19	1.57	0.79	0.79	0.25	0.60
MAC	10	3	5	50	2000	200	6	50	10	20	40	20			

city on the Gulf of Aqaba coast, at 28° 25' 28" N, 34° 45' 18" E (El-Sorogy et al., 2020; Fig. 1). The coastline in the study area is bounded by pre-Cambrian basement rocks and Tertiary and Quaternary sedimentary rocks. Thirty-three surface seawater samples were collected from the subtidal zone. Salinity, electrical conductivity, and pH were measured directly in situ for seawater. Cr, Co, Ni, Cu, Zn, Cd, Sb, As, Fe, Mn, Hg, and Pb were analyzed using inductively coupled plasma mass spectrometer (ICP-MS), NexION 300 D (Perkin Elmer, USA), at King Saud University. The ICP-MS was externally calibrated. The calibration curves of Cr, Cd, Cu, Pb, Co, and Ni were obtained using a blank and three working standards 0, 50, 100, and 200 µg/l (Panreac, 766333.1208). Sb and Zn were prepared from 1000 mg/l single standard solutions for ICP-MS (Aristar grade, BDH laboratory supplies, England for the trace elements). Calibration curves showed an excellent linearity for all elements. The seawater samples were diluted

10 times with deionized water prior to measurements. To assess pollution, water pollution index (PI<sub>j</sub>), degree of contamination (C<sub>d</sub>), and heavy metal pollution index (HPI) were used (Supplementary Table 1), and to identify the possible sources of HMs in the investigated seawaters, dendrograms using average linkage, principal component analysis, and Pearson’s correlation coefficient were conducted as statistical analyses, using SPSS 16.0 statistical software and Microsoft Excel 2016.

**Results and discussion**

**Concentration and distribution of HMS**

Supplementary Table 2 presents the coordinates of the sampling sites, pH, electrical conductivity, salinity, the HM values and the results of the

**Table 2** The correlation matrix of the investigated HMs

	As	Cd	Co	Cr	Cu	Fe	Hg	Mn	Pb	Sb	Zn	Ni	PI <sub>j</sub>	C <sub>d</sub>	HPI
As	1														
Cd	-.035	1													
Co	0.111	.138	1												
Cr	-.120	-.067	-.203	1											
Cu	0.944**	-.026	.139	-.155	1										
Fe	0.078	-.001	-.308	-.230	.051	1									
Hg	0.009	-.024	-.223	.292	.102	.072	1								
Mn	0.044	.172	-.045	.054	.109	-.285	.154	1							
Pb	-.044	-.214	-.108	.012	-.097	-.075	-.197	-.151	1						
Sb	-.050	.021	-.184	.235	-.026	.038	.260	.176	-.343	1					
Zn	0.119	.231	.043	.119	.115	.350*	.268	-.099	-.137	-.063	1				
Ni	0.033	-.309	-.116	.006	-.011	.010	-.123	-.036	.282	.193	-.002	1			
PI <sub>j</sub>	0.112	.138	1.000**	-.203	.140	-.308	-.223	-.045	-.107	-.184	.043	-.115	1		
C <sub>d</sub>	0.680**	-.054	.514**	-.148	.665**	-.110	-.131	-.008	.444**	-.233	.183	.262	.515**	1	
HPI	0.855**	.160	.474**	-.149	.809**	-.062	-.092	.051	.174	-.132	.210	.078	.475**	.918**	1

\*\*Correlation is significant at the 0.01 level

\*Correlation is significant at the 0.05 level

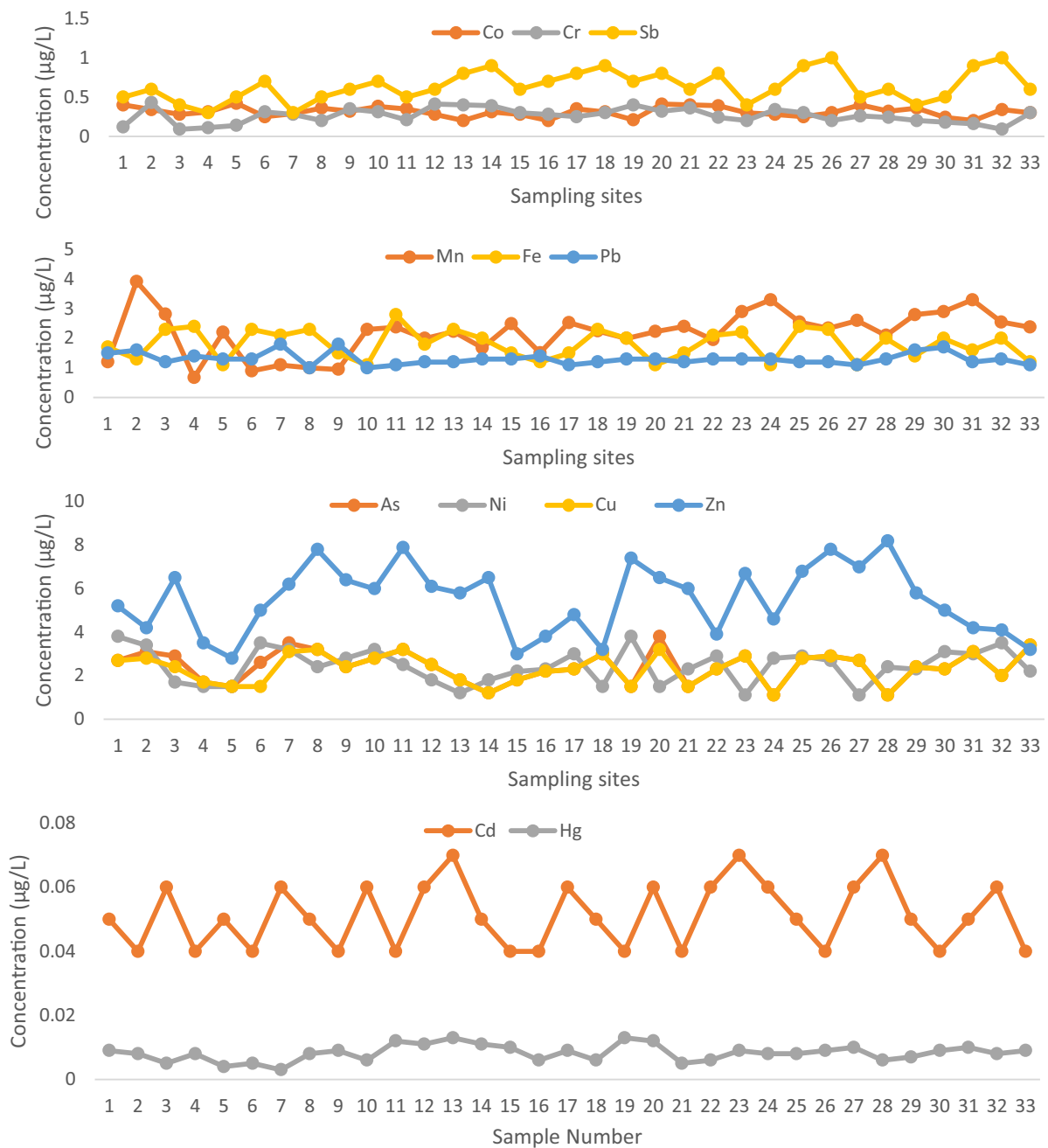


**Fig. 2** Spatial distribution of HMs in coastal seawaters from Gulf of Aqaba-Red Sea coastline, northwest Saudi Arabia

water pollution index (PI<sub>j</sub>), degree of contamination ( $C_d$ ), and heavy metal pollution index (HPI) of 33 surface seawater samples. Table 1 presents the minimum, maximum, mean and standard deviation of HMs, maximum admissible concentration (Siegel, 2002; WHO, 2011), and the applied

pollution indices. The HMS took the following order: Zn (mean 5.51 µg/L) > Ni (2.45) > As (2.43) > Cu (2.34) > Mn (2.20) > Fe (1.81) > Pb (1.31) > Sb (0.64) > Co (0.31) > Cr (0.26) > Cd (0.05) > Hg (0.008). The distribution of HMs shows a fluctuating pattern without fixed direction

**Table 3** Principal component loadings and explained variance for the six components with the varimax normalized rotation

	Component					
	1	2	3	4	5	6
As	.963	-.035	.007	.043	.017	-.057
Cd	.023	.149	-.683	.074	.029	.072
Co	.150	.960	-.109	-.003	-.039	-.132
Cr	-.170	-.071	.116	-.033	-.198	.794
Cu	.958	-.023	-.042	.103	-.021	-.041
Fe	.078	-.372	-.036	.151	.782	-.160
Hg	.074	-.229	-.135	.274	.055	.657
Mn	.166	-.120	-.225	.220	-.643	.154
Pb	.056	-.083	.387	-.820	-.054	.027
Sb	-.048	-.096	.297	.774	-.116	.242
Zn	.179	.123	-.227	.003	.658	.511
Ni	.079	.011	.828	.025	.072	.043
PI <sub>j</sub>	.152	.960	-.108	-.004	-.039	-.132
C <sub>d</sub>	.775	.441	.229	-.352	.028	.035
HPI	.901	.367	-.007	-.147	.017	.014
% of Variance	22.78	16.25	10.69	10.55	10.19	9.87
Cumulative %	22.78	39.02	49.71	60.27	70.45	80.32

(Fig. 2), but there were some sites characterized by higher HM levels, such as sites 1, 2, 5, 7, and 9 (Ni, Cr, Mn, Co, and Pb) and sites 11, 13, 19, 20, 23, 28, and 33 (Hg, As, Zn, Cd and Cu). Most of these sites are located nearby Sharma, Ras Hemaïd, and Magnah cities, indicating anthropogenic sources (El-Sorogy et al., 2020).

As shown in supplementary Table 3, the average Pb and Cd levels are lower than those reported from Caspian coast, Iran (Abadi et al., 2018), north Atlantic and North Pacific (Donat & Bruland, 1995), and Jazan coastline, Red Sea, and Saudi Arabia (Kahal et al., 2020). Zn and Ni are lower than those reported from Al-Khobar, Saudi Arabian Gulf (Alharbi et al., 2017; Alharbi & El-Sorogy, 2019) and Caspian coast, Iran (Abadi et al., 2018). On the other hand, average value of As is higher than those reported from Al-Khafji, Arabian Gulf (Alharbi & El-Sorogy, 2019), the Gulf of Aqaba (Shriadah et al., 2004), and Rosetta coast, Mediterranean Sea, and Egypt (El-Sorogy & Attiah, 2015). Furthermore, average Cd level is higher than those reported from the Gulf of Aqaba, Saudi Arabia (Al-Taani et al., 2014), and Tarut Island, Arabian Gulf (El-Sorogy et al., 2016).

**Pollution indices and multivariate analyses**

The spatial distribution of the water pollution index (PI<sub>j</sub>), degree of contamination (C<sub>d</sub>), and heavy metal pollution index (HPI) is mostly coinciding with the spatial distribution of heavy metals (Fig. 3), i.e., fluctuating with higher individual sites, mostly located nearby Sharma, Ras Hemaïd, and Magnah cities. PI<sub>j</sub> levels ranged from 2.01 in samples 13 and 16 to 4.22 in sample 5. All seawater samples were categorized as good water (1 ≤ PI<sub>j</sub> ≤ 5) (Tanjung et al., 2019). Levels of C<sub>d</sub> ranged from 1.95 in sample 13 to 2.91 in sample 7. The investigated samples are categorized as low pollution (C<sub>d</sub> < 4) (Backman et al., 1997). Based in classification illustrated in supplementary Table 1, levels of the heavy metal pollution index (HPI) ranged from 4.31 in sample 19 to 6.78 in sample 20. 30.30% (10 samples) are classified as low pollution (HPI < 5) and 69.7% (23 samples) fell under medium pollution (HPI = 5–10) (Prasanna et al., 2012).

Pearson’s correlation showed a strong correlation between Cu and As (r = 0.944), PI<sub>j</sub> and Co (r = 1.00), C<sub>d</sub> and Cu (r = 0.665), HPI, and each of As and C<sub>d</sub>

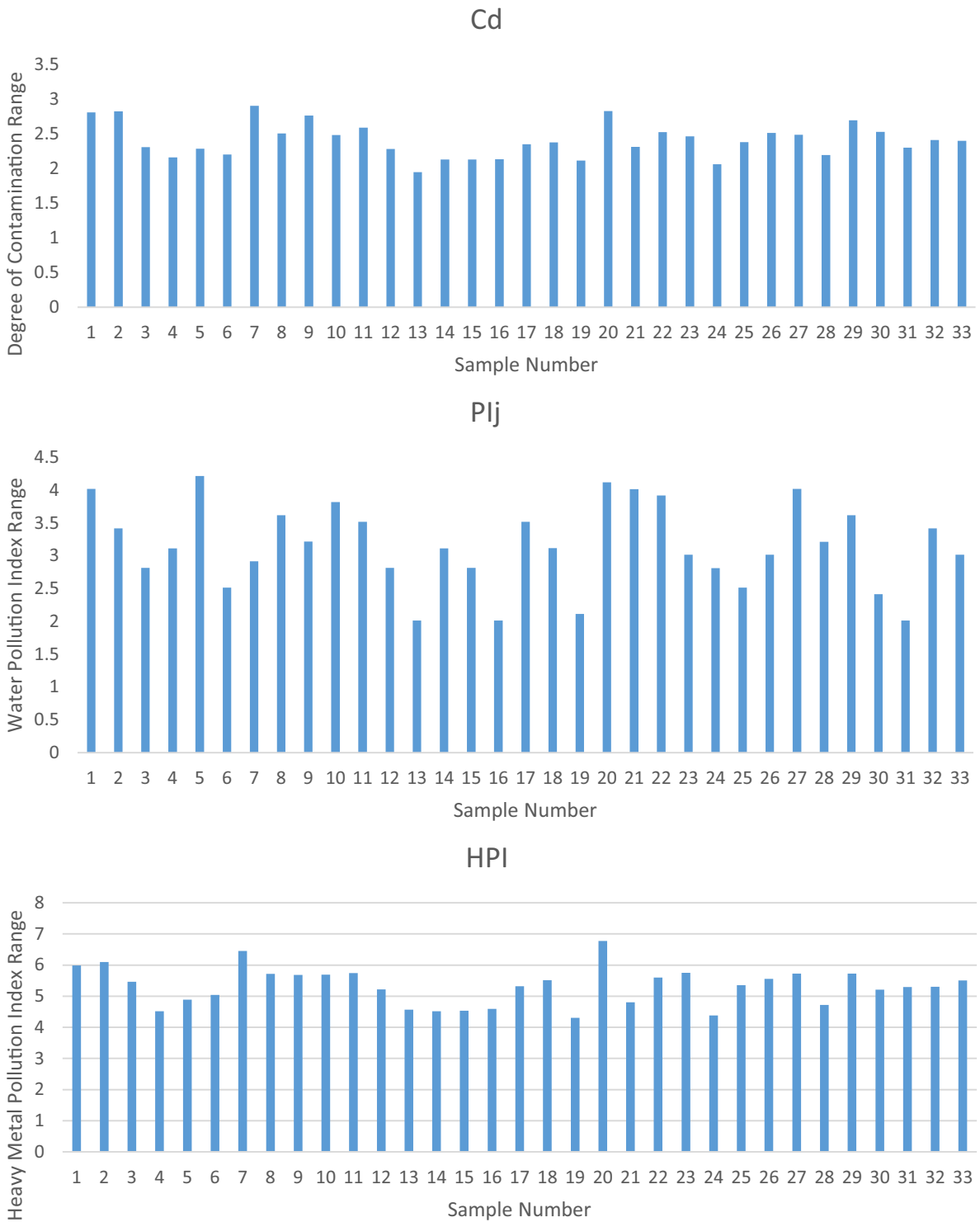


**Fig. 3** Spatial distribution of the water pollution index ( $PI_j$ ), degree of contamination ( $C_d$ ), and heavy metal pollution index (HPI) of the seawaters samples from the study area

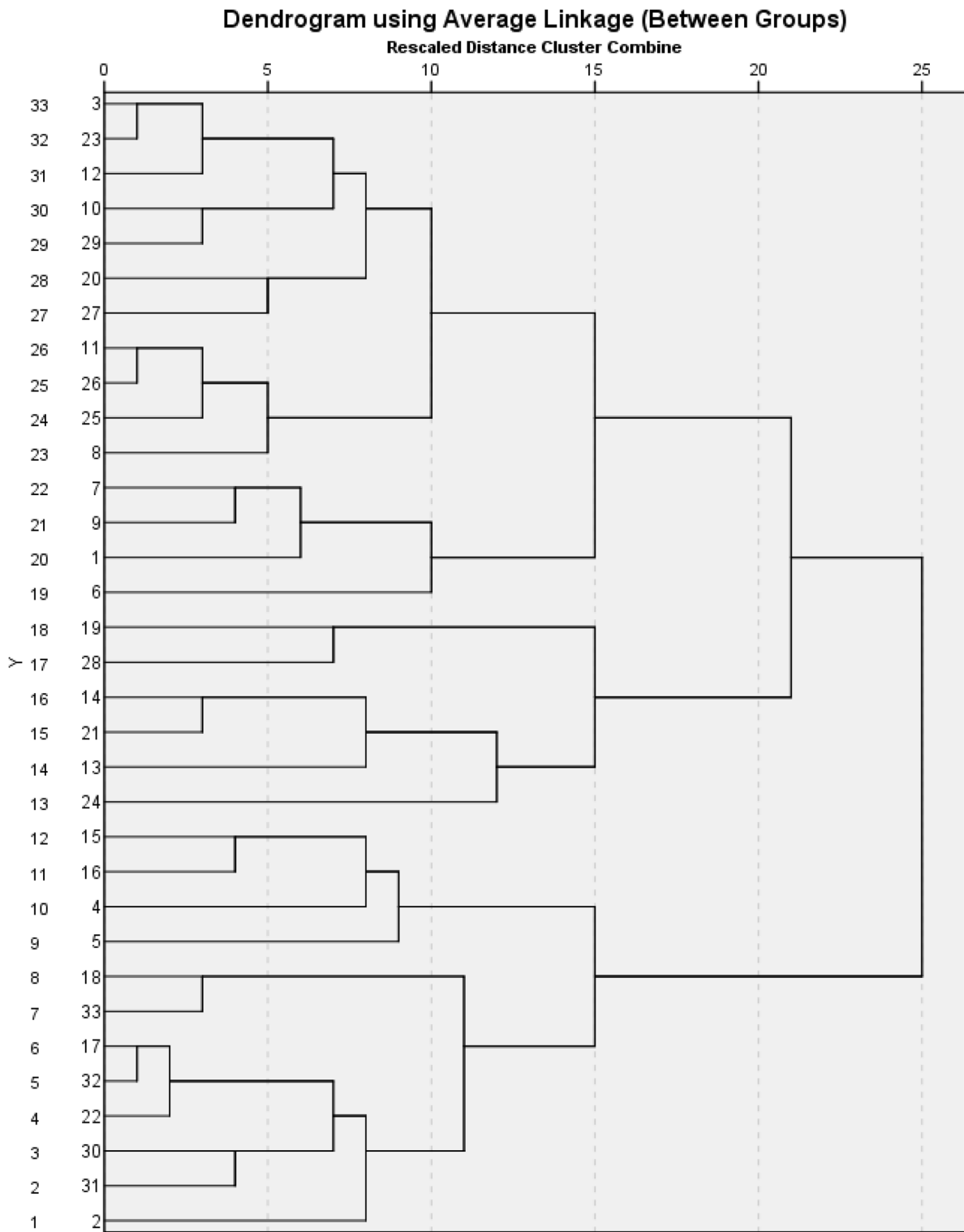


**Fig. 4** Dendrogram for hierarchal clusters analyses of 33 seawater samples from the Red Sea-Gulf of Aqaba coastline



( $r = 0.855$  and  $0.918$ , respectively, Table 2). All samples of the higher HPI,  $C_d$ , and  $PI_j$  levels reported higher concentrations of As, Cu, and Co, respectively (e.g., samples 1, 2, 5, 7, 20, 27, and 29). This indicated that the HPI,  $C_d$ , and  $PI_j$  levels are depended mainly on As, Cu, and Co levels, respectively. The possible natural sources of these HMs are rock weathering and volcanic eruptions, while the anthropogenic sources are petroleum refining, the agricultural applications such as herbicides, insecticides, algicides, fungicides, wood preservatives, sheep dips, and dye-stuffs (ATSDR, 2000; Tchounwou et al., 2012; Obinna & Ebere, 2019). Moreover, As is partially volatile during coal combustion (Tian et al., 2013). Negative correlations were observed between many HM pairs, such as Pb-As, Pb-Co, Pb-Cd, Pb-Cu, Pb-Fe, Pb-Hg, and Pb-Mn (Table 2). Moreover, negative correlations were reported between Ni-Cd, Ni-Co, Ni-Cu, Ni-Hg, Ni-Mn, and Ni-Zn. The lack of significant correlations between HM pairs implies various pollution sources (Chen et al., 2014; Alharbi & El-Sorogy, 2019).

The dendrogram of sample locations and HMs subdivided the studied localities at distance 25 into two clusters (Fig. 4). The first cluster is subdivided into four subclusters at distance 15 and contains samples (3, 23, 12, 10, 29, 20, 27, 11, 26, 25, and 8), (7, 9, 1, and 6), (19 and 28) and (14, 21, 13, and 24). Seawater samples in this cluster reported the highest values of As (sample 20), Fe (sample 11), Pb (sample 9), Sb (sample 26), Zn (sample 28), Cd (samples 13, 23, 28), Hg (samples 13, 19), Ni (sample 1),  $C_d$  (sample 7), and HPI (sample 20). The second cluster is subdivided into two groups and accounts samples (15, 16, 4, and 5) and (18, 33, 17, 32, 22, 30, 31, and 2). Seawater of this cluster includes the highest levels of Mn (sample 2), Cr (sample 2), Co (sample 5), Cu (sample 33), and  $PI_j$  (sample 5).

Six principal components, covering 80.32% of the total variance, were extracted (Table 3). Each group of elements possibly originates from similar sources. The first component covers 22.78% and presents a significant positive loading for As, Cu,  $C_d$ , and HPI (0.963, 0.958, 0.775, and 0.901, respectively), which derived mainly from geogenic source, from chemical weathering of the Pre-Cambrian basement, and Phanerozoic rocks bounded the Red Sea-Gulf of Aqaba coast. The second component covers 16.25% and presents positive loading for Co and  $PI_j$  (0.960 and 0.960, respectively), which related mostly to anthropogenic activities from industrial activities, traffic emissions, and the dredging

of the aquatic sediments. The third, fourth, and fifth components account 10.69, 10.55, and 10.19, respectively, and show positive loading in Ni, Sb, and Zn (0.828, 0.774, and 0.658), which may be indicated combined natural and anthropogenic sources for these heavy metals. The sixth component covers 9.87% and presents high positive loading for Cr, and Zn (0.794 and 0.511, respectively). The presence of Zn as positive loading in components fifth and sixth may be attributed to different sources for Zn in the investigated seawater. Finally, pollution indices and statistical analyses revealed that the quality of seawater in the Red Sea-Gulf of Aqaba coastline is mainly controlled by geogenic processes from chemical weathering of the nearby basement and sedimentary rocks, with minor anthropogenic input from industrial and agricultural applications.

## Conclusions

1. The average HM contents ( $\mu\text{g/l}$ ) in 33 seawater samples from the Red Sea-Gulf of Aqaba coastline were in the following order: Zn (5.51) > Ni (2.45) > As (2.43) > Cu (2.34) > Mn (2.20) > Fe (1.81) > Pb (1.31) > Sb (0.64) > Co (0.31) > Cr (0.26) > Cd (0.05) > Hg (0.01). Spatial distribution of HMs showed higher levels in sites near Sharma, Ras Hmaid, and Magnah cities.
2. All seawater samples were categorized as light and low polluted, according to  $PI_j$  and Cd, while 10 samples were low polluted and 23 ones were medium polluted, according to HPI. Most average HM levels were lower than those reported from many worldwide seawaters, except for As level, which is higher than those reported from Al-Khafji and the Gulf of Aqaba, and Rosetta coast, Mediterranean Sea, and Egypt. Also, Cd level is higher than those recorded from Tarut island and the Gulf of Aqaba.
3. Multivariate analyses subdivided the HMs into two large clusters and six principal components, which suggest different sources of pollutants. As, Cu, and Fe were derived from geogenic sources from the Pre-Cambrian basement and the Phanerozoic sedimentary rocks along the coast, while Co and Pb were derived from anthropogenic pollutants from urbanization and agricultural and industrial activities. Ni, Sb, and Zn were derived from combined lithogenic and anthropogenic sources.



**Supplementary information** The online version contains supplementary material available at <https://doi.org/10.1007/s10661-021-08911-8>.

**Acknowledgements** The authors would like to thank the anonymous reviewers for their valuable suggestions and constructive comments. The Deanship of Scientific Research, King Saud University, provided funding for this research group (No. RG-1435-033).

## References

- Abadi, M., Zamani, A., Parizanganeh, A., Khosravi, Y., & Badiie, H. (2018). Heavy metals and arsenic content in water along the southern Caspian coasts in Iran. *Environmental Science and Pollution Research*. <https://doi.org/10.1007/s11356-018-2455-7>.
- Agency for Toxic Substances and Disease Registry (ATSDR). (2000). *Toxicological profile for Arsenic TP-92/09*. Georgia: Center for disease control, Atlanta.
- Akif, M., Khan, A. R., Hussain, Z., Mall-Abrar, K., M., & Sok, K., Min, Z., Muhammad, A. (2002). Textile effluents and their contribution towards aquatic pollution in the Kabul River (Pakistan). *Journal of the Chemical Society of Pakistan*, 24(2), 106–111.
- Alharbi, T., Alfaifi, H., & El-Sorogy, A. S. (2017). Metal pollution in Al-Khobar seawater, Arabian Gulf, Saudi Arabia. *Marine Pollution Bulletin*, 119, 407–415.
- Alharbi, T., & El-Sorogy, A. S. (2019). Assessment of seawater pollution of the Al-Khafji coastal area, Arabian Gulf. *Saudi Arabia. Environmental Monitoring and Assessment*, 191, 383.
- Ali, H., Khan E., & Ilahi, I. (2019) Environmental chemistry and ecotoxicology of hazardous heavy metals: Environmental persistence, toxicity, and bioaccumulation Hindawi Journal of Chemistry. <https://doi.org/10.1155/2019/6730305>
- Al-Mur, B. A., Quicksall, A. N., & Al-Ansari, A. M. (2017). Spatial and temporal distribution of heavy metals in coastal core sediments from the Red Sea. *Saudi Arabia. Oceanologia*, 59(3), 262–270.
- Al-Sofyani, A. A., Marimuthu, N., & Wilson, J. J. (2014). A rapid assessment of scleractinian and non-Scleractinian coral growth forms along the Saudi Arabian coast, Red Sea. *Journal of Ocean University of China*, 13(2), 243–248.
- Al-Taani, A. A., Batayneh, A., Nazzal, Y., Ghrefat, H., Elawadi, E., & Zaman, H. (2014). Status of trace metals in surface seawater of the Gulf of Aqaba, Saudi Arabia. *Marine Pollution Bulletin*, 86, 582–590.
- Backman, B., Bodis, D., Lahermo, P., Rapant, S., & Tarvainen, T. (1997). Application of a groundwater contamination index in Finland and Slovakia. *Environmental Geology*, 36, 55–64.
- Badr, N. B., El-Fiky, A. A., Mostafa, A. R., & Al-Mur, B. A. (2009). Metal pollution records in core sediments of some Red Sea coastal areas, Kingdom of Saudi Arabia. *Environmental Monitoring and Assessment*, 155(1–4), 509–526.
- Bozkurt, E., Eliri, Ö., & Kesiktaş, M. (2014). Analysis of heavy metals in seawater samples collected from beaches of Asian side of Istanbul. *Journal of Recreation and Tourism Research*, 1(1), 39–47.
- Chen, H., Lu, X., & Li, L. Y. (2014). Spatial distribution and risk assessment of metals in dust based on samples from nursery and primary schools of Xi'an, China. *Atmospheric Environment*, 88, 172–182.
- Donat, J. R., & Bruland, K. W. (1995). Trace elements in the oceans. In B. Salbu & E. Steinnes (Eds.), *Trace elements in natural waters* (pp. 247–292). Boca Raton: CRC Press.
- Dossis, P., & Warren, L. J. (1980). Distribution of heavy metals between the minerals and organic debris in a contaminated marine sediment. In R. A. Baker (Ed.), *Contaminants and Sediments* (pp. 119–139). Ann Arbor: Ann Arbor Science Publishers.
- El-Sorogy, A., & Attiah, A. (2015). Assessment of metal contamination in coastal sediments, seawaters and bivalves of the Mediterranean Sea coast. *Egypt. Marine Pollution Bulletin*, 101, 867–871.
- El-Sorogy, A., Youssef, M., Al-Kahtany, Kh., & Saleh, M. M. (2020). *Distribution, source, contamination and ecological risk status of heavy metals in the Red Sea-Gulf of Aqaba coastal sediments*. Marine Pollution Bulletin (Accepted): Saudi Arabia.
- El-Sorogy, A. S., Youssef, M., & Al-Kahtany, Kh. (2016). Integrated assessment of the Tarut Island coast, Arabian Gulf. *Saudi Arabia. Environmental Earth Sciences*, 75, 1336.
- Ghandour, I. M., Basaham, S., Al-Washmi, A., & Masuda, H. (2014). Natural and anthropogenic controls on sediment composition of an arid coastal environment: Sharm Obhur, Red Sea. *Saudi Arabia. Environmental Monitoring and Assessment*, 186(3), 1465–1484.
- Kabata-Pendias, A. (2011). *Trace elements in soils and plants* (3rd ed., p. 331). Boca Raton. London New York Washington, D.C: CRC Press.
- Kahal, A., El-Sorogy, A. S., Alfaifi, H., Almadani, S., & Ghrefat, H. A. (2018). Spatial distribution and ecological risk assessment of the coastal surface sediments from the Red Sea, northwest Saudi Arabia. *Marine Pollution Bulletin*, 137, 198–208.
- Kahal, A., El-Sorogy, A. S., Qaysi, S., Almadani, S., Kassem, S. M., & Al-Dossari, A. (2020). Contamination and ecological risk assessment of the Red Sea coastal sediments, southwest Saudi Arabia. *Marine Pollution Bulletin*, 154, 111125.
- Karuppasamy, M., Qurban, M.A.B., Krishnakumar, P.K. (2019). Metal contamination assessment in the sediments of the Red Sea Coast of Saudi Arabia. In Oceanographic and biological aspects of the Red Sea (pp. 147–170). Springer, Cham. [https://doi.org/10.1007/978-3-319-99417-8\\_9](https://doi.org/10.1007/978-3-319-99417-8_9)
- Lian, M., Wang, J., Sun, L., Xu, Z., Tang, J., Yan, J., & Zeng, X. (2019). Profiles and potential health risks of heavy metals in soil and crops from the watershed of Xi River in Northeast China. *Ecotoxicology and Environmental Safety*, 169, 442–448.
- Louriño-Cabana, B., Lesven, L., Charriau, A., Billon, G., Ouddane, B., & Boughriet, A. (2011). Potential risks of metal toxicity in contaminated sediments of Deûle river in Northern France. *Journal of Hazardous Materials*, 186(2–3), 2129–2137.
- Obinna, I. B., & Ebere, E. C. (2019). A Review: Water pollution by heavy metal and organic pollutants: Brief review of sources, effects and progress on remediation with aquatic

- plants. *Analytical Methods in Environmental Chemistry Journal*, 2(3), 5–38.
- Pan, K., Lee, O. O., Qian, P. Y., & Wang, W. X. (2011). Sponges and sediments as monitoring tools of metal contamination in the eastern coast of the Red Sea. *Saudi Arabia. Mar Poll Bull*, 62(5), 1140–1146.
- Prasanna, M. V., Praveena, S. M., Chidambaram, S., Nagarajan, R., & Elayaraja, A. (2012). Evaluation of water quality pollution indices for heavy metal contamination monitoring: A case study from Curtin Lake, Miri City, East Malaysia. *Environmental Earth Sciences*, 67, 1987–2001.
- Qin, H., Su, Q., Khu, S., & Tang, N. (2014). Water quality changes during rapid urbanization in the Shenzhen River Catchment: An integrated view of socio-economic and infrastructure development. *Sustainability*, 6, 7433–7451.
- Rezania, S., Taib, S. M., Md Din, M. F., Dahalan, F. A., & Kamyab, H. (2016). Comprehensive review on phytotechnology: Heavy metals removal by diverse aquatic plants species from Wastewater. *Journal of Hazardous Materials*, 318, 587–599.
- Shi, Z., Qin, Sh., Zhang, Ch., Chiu, Y., Zhang, L. (2020). The impacts of water pollution emissions on public health in 30 provinces of China. *Healthcare* 8, 119, <https://doi.org/10.3390/healthcare8020119>.
- Shriadah, M. A., Okbah, M. A., & El-Deek, M. S. (2004). Trace metals in the water columns of the Red Sea and the Gulf of Aqaba. *Egypt. Water Air Soil Pollution*, 153, 115–124.
- Siegel, F. R. (2002). *Environmental geochemistry of potentially toxic metals*. Berlin: Springer.
- Tanjung, R. H. R., Hamuna, B., & Alianto, . (2019). Assessment of water quality and pollution index in coastal waters of Mimika. *Indonesia. Journal of Ecological Engineering*, 20(2), 87–94.
- Tchounwou, P. B., Yedjou, C. G., Patlolla, A. K., & Sutton, D. J. (2012). Heavy metals toxicity and the environment. *National Institute of Health*, 101, 133–164. [https://doi.org/10.1007/978-3-7643-8340-4\\_6](https://doi.org/10.1007/978-3-7643-8340-4_6).
- Tian, H. Z., Lu, L. H., & J.M., Gao, J.J., Cheng, K., Liu, K. Y., Qiu, P. P., Zhu, C. Y. (2013). A review of key hazardous trace elements in Chinese coals: Abundance, occurrence, behavior during coal combustion and their environmental impacts. *Energy & Fuels*, 27(2), 601–614.
- World Health Organization (WHO). (2011). *Guidelines for drinking-water quality* (4th ed.). Switzerland: Geneva.
- Youssef, M., & El-Sorogy, A. S. (2016). Environmental assessment of heavy metal contamination in bottom sediments of Al-Kharrar lagoon, Rabigh, Red Sea. *Saudi Arabian Journal of Geosciences*, 9, 474.
- Youssef, M., El-Sorogy, A. S., Osman, M., Ghandour, I., & Manaa, A. (2020). Distribution and metal contamination in core sediments from the North Al-Wajh area, Red Sea. *Saudi Arabia. Mar Poll Bull*, 152, 110924.

**Publisher's Note** Springer Nature remains neutral with regard to jurisdictional claims in published maps and institutional affiliations.